Competition between multiphoton/tunnel ionization and filamentation induced by powerful femtosecond laser pulses in air

W. Liu, Q. Luo, and S. L. Chin

Department de physique, de génie physique et d'optique and Centre d'optique, photonique et laser (COPL), Université Laval, Québec (Québec), Canada G1K 7P4

Received November 8, 2002

In this work we present experiments by focusing 42 femtosecond laser pulses in air using three different focal length lenses: f=100, 30 and 5 cm. For the longest focal length, only the filament, which is a weak plasma column, is observed. When the shorter focal length lens is used, a high density plasma is generated near the geometrical focus and coexists with a weak plasma channel of the filament. Under the tightest focusing condition, filamentation is prevented and only a strong plasma volume appears at the geometrical focus.

OCIS codes: 320.7120, 320.7150, 300.2530, 020.4180.

It is well known that when powerful ultrashort laser pulses propagate in optical media, filamentation occurs[1−8]. Due to its potential applications, such as writing waveguides in condensed matters[9,10], lightning discharge control[11] and remote sensing in air[12], the filamentation phenomenon has been extensively studied in recent years. During the propagation in different transparent optical media, self-focusing of the pulse occurs in the form of a series of self-foci giving a perception of a filament of light[13]. Each self-focusing process is balanced by the de-focusing effect of a plasma which is formed when the intensity at the self-focal region is sufficiently high to induce tunnel/multiphoton ionization in gases[2,3,14] or multiphoton excitation of electrons from the valence band to the conduction band in condensed matters[4]. This balance results in an upper limit in intensity inside the focal region and is called intensity clamping[14−16]. In fact, R. Sauerbrey in Jena, Germany was the first to have predicted this clamping effect (private communication, unpublished, 1993). The plasma density is thus limited due to this balancing act. The weak plasma column left behind by the continuous series of self-foci is called a filament. During the laser-material interaction process, self-phase modulation and self-steepening will widely broaden the laser spectrum, which can extend from the near infrared to ultraviolet. The consequence is a white light laser pulse (supercontinuum)[17,18].

We note that the self-focusing/filamentation process depends on the power of the laser pulse. The critical power of self-focusing differs from material to material. If the ultrashort laser pulse is focused by a lens, the leading part of the laser pulse whose power is below the critical power will undergo geometrical focusing and be concentrated to the geometrical focus. Thus the intensity at the geometrical focus will mainly depend on the focal length of the lens. Recently, both experimental results and numerical simulations[19], using water as an example of condensed matters, show that the shorter the focal length is, the higher is the intensity at geometrical focus, and the higher is the electron density. The high electron density at the geometrical focus may lead to the appearance of breakdown in water. Thus the competition between breakdown and filamentation shows up: long focal length lens will favor filamentation while with tight focusing, optical breakdown will precede and even suppress filamentation. In the intermediate condition, filamentation and optical breakdown coexist.

In principle, this external focal length dependent intensity at the geometrical focus should also be found in gases. Previous work has observed similar competition behavior as in water between filamentation and breakdown in high-pressure (20-atmosphere) CO_2 gas[20]. But in the femtosecond laser field and relatively low-pressure gases (for example in air), the laser pulse duration is shorter than the electron collisional time, which is of the order of one picosecond. Thus during the laser-air interaction, cascade ionization caused by collision can be neglected. If we confine the term *optical breakdown* to high electron density resulted from cascade ionization, no breakdown can be expected during the interaction of femtosecond laser pulse with low-pressure gases. The laser induced plasma will be principally due to multiphoton/tunnel ionization. In this letter, we present experimental results of using different focal length lenses to focus ultrashort laser pulses in air; laser induced plasma is found to pass from a single weak plasma column or filament, through the coexistence of a filament and a high density plasma at the geometrical focus, into one with only a high density plasma occurring around the geometrical focus.

Our femtosecond CPA laser system built by Spectra Physics/Positive light gives out three beams of pulses all with 40 − 50 fs duration: 1 kHz/2 mJ per pulse, 10 Hz/14 mJ per pulse and 10 Hz/100 mJ per pulse. This experiment used the second beam coming out of a two passes amplifier followed by a portable compressor. The output of the compressor is centered at 810 nm, with 0.8 cm diameter at $1/e^2$ and a 42-fs pulse duration (measured by Positive Light single shot autocorrelator). A half wave plate and a polarizer are located before the two passes amplifier to change the input seed beam power and thus change the output power of the compressor. The output of the compressor was focused by a lens in air. From

the side perpendicular to the laser propagation axis, the focal region was imaged by two fused silica lenses (both focal lengths are 5 cm) onto to the slit of a spectrometer (Acton SpectraPro 150). The magnification is 1/10. The silt was parallel to the laser propagation direction. The spectrometer has two interchangeable gratings, 1200 and 150 g/mm, and it is also armed with 1152 × 298 pixels, 16 bits CCD. We recorded the images of the focusing region by taking the zeroth order images; we also measured the spectral distribution of this region. Several different focal length lenses were used. In this paper, we report typical results using lenses with the following focal lengths: 100, 30 and 5 cm.

Figure 1 shows three typical images taken via the zeroth order grating dispersion . All the images were taken at 5 mJ/pulse input energy using the three lenses: (a) f=100 cm; (b) f=30 cm; (c) f=5 cm. The laser pulses propagate from the bottom to the top of the image. When f=100 cm lens was used, a long clean thin line was recorded in Fig. 1(a). The maximum signal along this line almost does not change. Because of the limit of the view area, the lower part of the line, which is closer to the focusing lens, was not imaged on the CCD. The signal coming from the thin line is so weak that a large contrast has to be applied in Fig. 1(a) to show it clearly. Figure 1(b) was taken at the same contrast as Fig. 1(a) when f = 30 cm was used. Not only a thin line but also a much brighter volume appears in the picture. The bright volume is at the geometrical focus. The maximum signal along the thin line is also constant. In the inset of Fig. 1(b), the same picture is shown using low contrast, where only a bright elongated volume is shown around the geometrical focus. Finally, when the lens' focal length is changed to 5 cm, corresponding to Fig. 1(c) only the bright volume around the geometrical focus can be seen clearly. The same contrast as Fig. 1(a) and Fig. 1(b) is adapted in Fig. 1(c). Similar to Fig. 1(b), the inset of Fig. 1(c) shows the picture at low contrast. Up to the CCD limitation, no elongation of the image is found in Fig. 1(c).

To take the spectra, we used the 150-g/mm grating inside the spectrometer to obtain a large spectral range from 300 to 1050 nm. Because of the response efficiency of the grating, the spectra below 300 nm cannot be detected. The spectrometer slit was open to 50 μm, which corresponds to the resolution of 4 nm. The spectra obtained are shown in Fig. 2 for the three lenses respectively. For all lenses, the spectra were taken at 5 mJ/pulse.

The results with the f=100 cm lens are shown in Fig. 2(a). The signal was accumulated by 200 laser shots. Several spectral lines spread around 350 nm. Because of the low resolution of the 150 g/mm grating, some of the lines cannot be distinguished in Fig. 2(a). The inset of Fig. 2(a) gives the fine spectrum from 300 to 450 nm taken by the 1200 g/mm grating, which has a high resolution of 0.4 nm. These lines have been assigned to be nitrogen molecules and ions fluorescence[21−23]. The scattered laser spectrum is shown at the longer wavelength side. There is almost no continuum spectrum shown in Fig. 2(a).

Figure 2(b) shows the spectra using the f=30 cm lens. The same accumulation time for the signal as above was

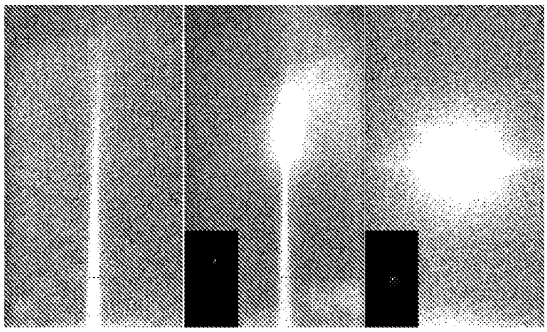

Fig. 1. Images taken via grating zero order at 5 mJ/pulse input energy. (a) f=100 cm, (b) f=30 cm, (c) f=5 cm. Inset: low contrast pictures of f=30 cm and f=5 cm.

applied. The spectra change obviously from Fig. 2(a) to Fig. 2(b). Though the molecular lines still can be observed, several lines around 800 nm start to show up. These lines can be identified as O and N atomic lines[24]. The strongest is found to be the O^1 line at 777.4 nm. Another clear change is that the continuum spectrum becomes obvious.

Figure 2(c) corresponds to the case of f=5 cm. Due to the very strong signal level, the spectra were taken by accumulating only 6 shots. The dramatic change is that no more nitrogen molecular lines are observed in Fig. 2(c), while the continuum becomes very strong. Meanwhile the continuum spectrum is modulated by strong O and N atomic lines around 800 nm. The stronger lines are N^1 (746.6 nm), O^1 (777.4 nm), O^1 (822.7 nm) and N^1 (868.6 nm). Again, because of the low resolution used

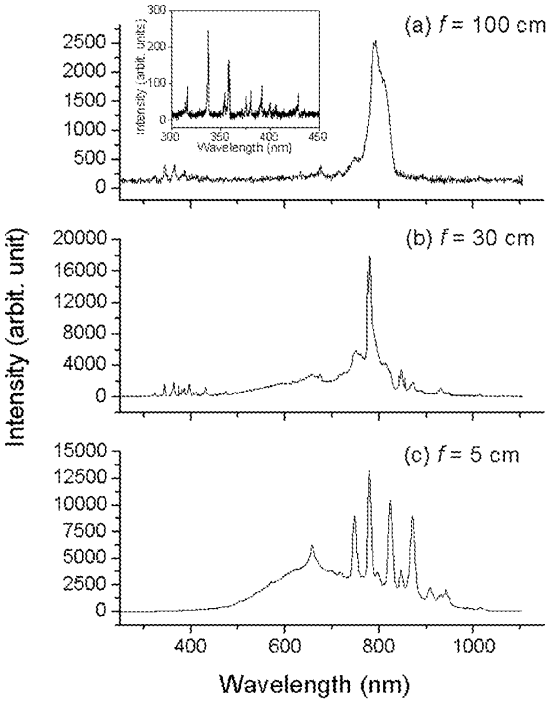

Fig. 2. Fluorescence spectra at 5 mJ/pulse input energy. (a) f=100 cm, (b) f=30 cm, (c) f=5 cm. Inset: high resolution spectrum around 350 nm when f=100 cm lens was used.

in our experiments, the atomic lines are broadened and some of them merge together.

To explain the experimental results, we remind ourselves some well-known interaction processes between ultrashort laser pulse and simple molecules[25,26]. In the strong laser field, air molecules are firstly ionized, i.e.

$$N_2 \rightarrow N_2^+ + e, \quad O_2 \rightarrow O_2^+ + e. \tag{1}$$

Further dissociation through bond softening would happen in our laser intensity range

$$N_2^+ \rightarrow N + N^+, \quad O_2^+ \rightarrow O + O^+. \tag{2}$$

The respective ionization potentials of these particles are 15.6 eV of N_2, 12.1 eV of O_2; and 14.5 eV of N, 13.6 eV of O. Once process (2) happens, O and N atoms might also be ionized with high probability as bellow

$$N \rightarrow N^+ + e, \quad O \rightarrow O^+ + e. \tag{3}$$

Because of the lack of collision as well as the much higher ionization potentials (O^+: 35.1 eV; N^+: 29.6 eV), O^+ and N^+ have very rare probability to be further ionized. After the laser pulse is gone, electrons will recombine with atomic and molecular ions. They would emit a continuum spectrum. Further down in the recombination energy ladder, molecules and atoms will decay to some radiative excited states where fluorescence is emitted.

In air, the intensity inside a filament is clamped down to $(4-6)\times 10^{13}$ W/cm^2, which gives a $10^{14}-10^{15}$ cm^{-3} plasma density[14,21,22]. The latter low plasma (electron) density indicates that process (1) is the main channel of interaction. This results in mainly fluorescence from excited nitrogen molecules and molecular ions and the background continuum is negligible[21–23,27,28]. The above result is reproduced in Fig. 2(a), where f=100 cm lens was used. It convinces us that the long thin line in Fig. 1(a) indicates a filament.

Conversely, in Fig. 2(c) no nitrogen molecular lines are observed. The spectrum consists of strong atomic lines and strong broad continuum. It hints that processes (2) and (3) have much higher probability to happen than that in the case of long focal length. Thus most of the molecules are dissociated, and much more excited atoms are produced via electron-atomic ions recombination. The appearance of high electron density is indicated by Fig. 1(c) in which the much brighter volume replaces the weak thin line in Fig. 1(a).

We calculate the distance between the position of the first self-focusing point (or the beginning of the filament) and the geometrical focus $d = f - z'_{\rm sf}$. $z'_{\rm sf}$ denotes the distance between the self-focus and the lens, and is given by[5]

$$z'_{\rm sf} = \frac{z_{\rm sf} f}{z_{\rm sf} + f}, \tag{4}$$

where $z_{\rm sf}$ is the self-focus of a parallel Gaussian input beam and determined by[29]

$$z_{\rm sf} = \frac{0.367ka^2}{\{[(\frac{P}{P_{\rm crit}})^{1/2} - 0.852]^2 - 0.0219\}^{1/2}}, \tag{5}$$

where k is the wave number, a is the initial laser beam radius at $1/e^2$ level, P is the laser peak power, and $P_{\rm crit}$ indicates the critical power of self-focus. For f=5 cm, d is found to be equal to 0.3 mm; i.e. the beginning of the self-focusing point almost coincides with the geometrical focus. Since filamentation is a propagation effect, there is no chance for the filament to develop before the high intensity in the focal region generates a strong plasma. The latter defocuses the rest of the pulse. No balance between the self-focusing and plasma defocusing effect can be established any more. Geometrical focusing plays a main role to focus the laser pulse and induce a very high intensity. Hence no filament can be seen in Fig. 1(c) and no nitrogen fluorescence coming from a filament can be observed in Fig. 2(c).

In the intermediate case, all the molecular lines, atomic lines and continuum are found in Fig. 2(b) (f=30 cm). Also Fig. 1(b) shows the coexistence of a filament (weak plasma column) and high density plasma around the geometrical focus. In this case, the distance between the self-focus and the geometrical focus is estimated to be 1 cm. This provides enough propagation distance to partially form a filament before the strong ionization in the geometrical focus takes over, as shown in Fig. 1(b).

In conclusion, when an ultrashort laser pulse is focused by a lens in air, filamentation and strong field ionization around the geometrical focus compete with each other. Only weak focusing condition can give rise to the pure filamentation. Coexistence of filamentation and strong field ionization in the geometrical focus results if a shorter focal length is used. In particular, if the focal length is so short that the self-focus occurs too close to the geometrical focus, filamenation is prevented by the strong plasma in the geometrical focus.

W. Liu's e-mail address is wliu@phy.ulaval.ca.

References

1. E. Yablonovitch and N. Bloembergen, Phys. Rev. Lett. **29,** 907 (1972).
2. N. Aközbek, C. M. Bowden, A. Talebpour, and S. L. Chin, Phys. Rev. E **61,** 4540 (2000).
3. A. Braun, G. Korn, X. Liu, D. Du, J. Squier, and G. Mourou, Opt. Lett. **20,** 73 (1995).
4. A. Brodeur and S. L. Chin, Phys. Rev. Lett. **80,** 4406 (1998).
5. A. Brodeur and S. L. Chin, J. Opt. Soc. Am. B **16,** 637 (1999).
6. E. T. J. Nibbering, M. Franco, B. S. Prade, G. Grillon, C. LeBlanc, and A. Mysyrowicz, Opt. Comm. **119,** 479 (1995).
7. R. Rairoux, H. Schillinger, S. Niedermeier, M. Rodriguez, F. Ronneberger, R. Sauerbrey, B. Stein, D. Waite, C. Wedekind, H. Wille, L. Wöste, and C. Ziener, Appl. Phys. B **71,** 573 (2000).
8. J. Kasparian, R. Sauerbrey, D. Mondelain, S. Niedermeier, J. Yu, J.-P. Wolf, Y.-B. André, M. Franco, B. Prade, S. Tzortzakis, A. Mysyrowicz, M.Rodriguez, H. Wille, and L. Wöste, Opt. Lett. **25,** 1397 (2000).
9. L. Sudrie, M. Franco, B. Prade, and A. Mysyrowicz, Opt. Comm. **191,** 333 (2001).
10. K. Yamada, W. Watanabe, T. Toma, K. Itoh, and J. Nishii, Opt. Lett. **26,** 19 (2001).
11. M. Rodriguez, R. Sauerbrey, H. Wille, L. Wöste, T. Fujii, Y.-B. André, A. Mysyrowicz, L. Klingbeil, K. Rethmeier, W. Kalkner, J. Kasparian, E. Salmon, J. Yu,

and J.-P. Wolf, Opt. Lett. **27,** 772 (2002).
12. P. Rairoux, H. Schillinger, S. Niedermeier, M. Rodriquez, F. Ronneberger, R. Sauerbrey, B. Steinl, and D. Waite, Appl. Phys. B **71,** 573 (2000).
13. A. Brodeur, C. Y. Chien, F. A. Ilkov, and S. L. Chin, Opt. Lett. **22,**304 (1997).
14. J. Kasparian, R. Sauerbrey, and S. L. Chin, Appl. Phys. B **71,** 877 (2000).
15. A. Becker, N. Akozbek, K. Vijayalakshmi, E. Oral, C. M. Bowden, and S. L. Chin, Appl. Phys. B **73,** 287 (2001).
16. W. Liu, S. Petit, A. Becker, N. Aközbek, C. M. Bowden, and S. L. Chin, Opt. Commun. **202,**189 (2002).
17. R. R. Alfano (ed.), *The Supercontinuum Laser Source* (New York, Springer, 1989).
18. S. L. Chin, A. Brodeur, S. Petit, O. G. Kosareva, and V. P. Kandidov, J. Nonlinear Opt. Phys. Mat. **8,** 121 (1999).
19. W. Liu, O. Kosareva, I. S. Golubtsov, A. Iwasaki, A. Becker, V.P. Kandidov, and S.L. Chin., Appl. Phys. B, **75,** 595 (2002).
20. F. A. Ilkov, L. Sh. Ilkova, and S.L. Chin, Opt. Lett. **18,** 681 (1993).
21. A. Talebpour, M. Abdel-Fattah, and S. L. Chin, Opt. Commun. **183,** 479 (2000).
22. A. Talebpour, M. Abdel-Fattah, A. D. Bandrauk, and S. L. Chin, Laser Phys. **11,** 68 (2001).
23. A. Talebpour, S. Petit, and S. L. Chin, Opt. Commun. **129,** 285 (1999).
24. National Institute of Standards and Technology online database, http://www.nist.gov/srd/atomic.htm.
25. A. Talebpour, J. Yang, and S. L. Chin, Opt. Commun. **163,** 29 (1999).
26. A. Talebpour, S. Larochelle, and S. L. Chin, Phys. B: At. Mol. Opt. Phys. **30,** 1927 (1997).
27. J. Yu, D. Mondelain, G. Ange, R. Volk, S. Niedermeier, J. P. Wolf, J. Kasparian, and R. Sauerbrey, Opt. Lett. **26,** 533 (2001).
28. N. Aközbek, M. Scalora, C. M. Bowden, and S. L. Chin, Opt. Commun. **191,** 353 (2001).
29. J. H. Marburger, Prog. Quantum Electron. **4,** 35 (1975).